F. King, Compiler (Report 9, Memorial University of Newfoundland, St. John's, 1982), p. 125; S. O'Brien and A. F. King, *ibid.*, p. 1.

11. H. Williams, Compiler, *Tectonic Lithofacies Map of the Appalachian Orogen* (Memorial University of Newfoundland, St. John's, 1978).
12. J. Rodgers, *Am. J. Sci.* **272**, 507 (1972); L. Glover III and A. K. Sinha, *ibid.* **273-A**, 234 (Abstr.) (1973); C. A. Kay and R. E. Zartman, *Va. Polytech. Inst. State Univ. Dep. of Geol. Sci. Mem. 2* (1980), p. 257.
13. A. A. Stromquist and H. W. Sundelius, *U.S. Geol. Surv. Bull. 1274-B* (1969).
14. D. T. Secor, Jr., *et al.*, *J. Geophys. Res.* **87**, 6974 (1982).
15. J. R. Butler and P. D. Fullagar, *Geol. Soc. Am. Bull.* **89**, 460 (1978); P. D. Fullagar, *S.C. Geol. Surv.* **25**, 29 (1981).
16. J. F. Sutter, D. J. Milton, M. J. Funk, *Geol. Soc. Am. Abstr. Programs* **15**, 110 (1983).
17. S. A. Kish *et al.*, *ibid.* **11**, 184 (1979).
18. H. Williams, in *Structural Map of the Appalachian Orogen in Canada*, J. D. Keppie, Coordinator, (Map No. 4, Memorial University of Newfoundland, St. John's, 1978); J. D. Keppie, *ibid.*
19. A. W. Snoke, S. A. Kish, D. T. Secor, Jr., *Am. J. Sci.* **280**, 1018, (1980).
20. J. Pindell and J. F. Dewey, *Tectonics* **1**, 179 (1982).
21. J. W. Skehan and D. P. Murray, *Tectonophysics* **69**, 285 (1980).
22. N. Rast and R. Grant, *Am. J. Sci.* **273**, 572 (1973).
23. B. B. Ellwood, *J. Geophys. Res.* **87**, 5339 (1982); C. Barton and L. Brown, *ibid.* **88**, 2327 (1983); R. E. Dooley, *Phys. Earth Planet. Inter.* **31**, 241 (1983).
24. D. V. Kent, *J. Geophys. Res.* **87**, 8709 (1982).
25. Supported by NSF grant EAR 80-20474. We benefitted from discussions and reviews by numerous colleagues. A representative collection of the trilobites described herein will be donated to the U.S. National Museum.

7 March 1983; revised 18 May 1983

Martian Gases in an Antarctic Meteorite?

Abstract. *Significant abundances of trapped argon, krypton, and xenon have been measured in shock-altered phases of the achondritic meteorite Elephant Moraine 79001 from Antarctica. The relative elemental abundances, the high ratios of argon-40 to argon-36 (≥ 2000), and the high ratios of xenon-129 to xenon-132 (≥ 2.0) of the trapped gas more closely resemble Viking data for the martian atmosphere than data for noble gas components typically found in meteorites. These findings support earlier suggestions, made on the basis of geochemical evidence, that shergottites and related rare meteorites may have originated from the planet Mars.*

Achondrites are differentiated meteorites believed to have formed by igneous processes on their original parent bodies. Three groups of rare achondrites, the shergottites, nakhlites, and chassignites (SNC meteorites) differ from other achondrites in several important aspects. They generally show a higher oxidation state, are unbrecciated, have more complex abundance patterns of rare-earth elements, and have distinctly different values of certain diagnostic chemical ratios such as K/U and La/W (*1*, *2*). The isotopic composition of oxygen also differs subtly among the SNC meteorites, other achondrites, and Earth (*3*). The igneous formation ages of all SNC meteorites are about 1300 million years, which is far younger than the ages of any other known extraterrestrial material (including lunar rocks), and implies geologically recent igneous activity (*4*–*6*). These properties have led several investigators to conclude that these meteorites must have formed on a geologically complex and relatively large parent body, most probably the planet Mars (*2*, *4*, *5*, *7*–*9*).

The Allan Hills (ALH77005) and Elephant Moraine (EET79001) shergottites were recently recovered from the Antarctic ice sheet (*10*). Both closely resemble two known shergottites (*4*, *8*, *11*, *12*). All shergottites have experienced impact shock, whereas the nakhlites show essentially no evidence of shock. The time of this shock event in all four shergottites is determined by their rubidium-strontium isochron ages to have been approximately 180 million years ago (*4*, *12*) and probably coincides with the time when the shergottites were ejected from their parent body by a large-scale impact. The EET79001 meteorite is composed of two distinct igneous lithologies and has abundant shock-glass veins and inclusions probably formed during the dated shock event (*11*, *13*). The compositions of shock glass differ in the two lithologies, probably reflecting the effects of localized melting (*11*).

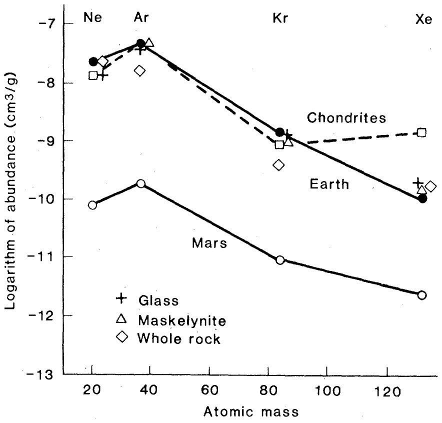

Fig. 1. Elemental concentrations of neon, argon (^{36}Ar + ^{38}Ar), krypton, and xenon of the EET79001 meteorite. The values for Earth (●) are the atmospheric abundances divided by the mass of the Earth minus the core. The values for Mars (○) are the atmospheric abundances divided by the mass of Mars (*15*). The $^{36+38}$Ar concentrations of chondrites typically lie in the range 0.5×10^{-8} to 100×10^{-8} cm^3/g, and we have arbitrarily normalized chondritic argon to the terrestrial value. Elemental ratios for chondrites (□) are from Mazor *et al.* (*24*). Those few achondrites that contain trapped gases either show an abundance pattern like that of chondrites (ureilites) or contain a helium- and neon-rich component implanted by the solar wind.

Our attempts to measure the potassium-argon age of EET79001 had indicated the presence of a trapped argon component. To determine the nature of these trapped noble gases, we measured the isotopic compositions by mass spectrometry of all five noble gases (helium, neon, argon, krypton, and xenon) in unirradiated whole-rock samples of both igneous lithologies of EET79001, in two shock-glass inclusions from the major lithology (lith-A), and in a ~ 98 percent pure feldspar separate prepared from the minor lithology (lith-B). Stepwise temperature extractions were made on all samples to better separate low-temperature, adsorbed terrestrial atmospheric gases from trapped gases and from gases produced by nuclear processes. Both glass samples, the feldspar, and lith-B whole rock (containing glass) released gases primarily near sample melting at 1100° to 1300°C. Trapped neon apparently was also released from these samples, but the larger neon system blank makes the neon concentrations considerably more uncertain. Total concentrations of ^{36}Ar released were 1×10^{-8} to 4×10^{-8} cm^3 STP/g (STP = standard temperature and pressure), which is ~ 10 to 20 times the ^{36}Ar produced in EET79001 by cosmic-ray interactions. A pyroxene separate and a total melt extraction of lith-A whole rock, however, gave ^{36}Ar concentrations that were lower by factors of ~ 42 and ~ 7, respectively. Those EET79001 samples containing trapped gases also contained ^{40}Ar far in excess of the amounts that could have formed in situ during the past 180 million years, the time of complete shock resetting of the rubidium-strontium ages, or during the past 1300 million years, the probable formation age of the meteorite (*4*, *12*). For example, one glass sample contained ~ 400 and ~ 40 times the amount of ^{40}Ar that could have formed in situ in 180 and 1300 million years, respectively (*14*).

The relative abundances of trapped neon, argon, krypton, and xenon in various EET79001 samples closely resemble those found in the atmospheres of Earth and Mars, but Kr/Xe ratios in these samples are distinct from that in chondrites (Fig. 1). The plotted values for Earth and Mars probably represent lower limits to the noble gas concentrations of the silicate material which accreted these planets because of possible incom-

Table 1. Evaluation of four possible origins of noble gas components in the EET79001 meteorite.

Characteristic of EET79001 noble gases	Consistent with origin from			
	Martian atmosphere	Chondritic contaminant	Terrestrial atmosphere (adsorbed)	Achondritic parent
Relative gas abundances	Yes	No	Unlikely	Unlikely
Trapped argon component with $^{40}Ar/^{36}Ar > 2000$	Yes	Maybe	No	Unlikely
Low $^{4}He/^{40}Ar$	Maybe	Unlikely	Yes	Unlikely
Trapped xenon with $^{129}Xe/^{132}Xe \geq 2$; no excess ^{129}Xe in lith-A whole rock	Yes	Unlikely	No	No
Neutron-capture component	Maybe	Maybe	No	Unlikely

plete degassing. The average Kr/Xe ratio of four EET79001 samples is 8; the terrestrial atmospheric value is 13; the chondritic value is 0.6; and the martian atmospheric value is ~ 4 but may be somewhat higher (*15*, *16*). This difference in Kr/Xe between the planets and chondrites commonly has been attributed to the distortion of a chondrite-like pattern by the incorporation of xenon into sediments on Earth and Mars (*17*). It is also possible, however, that both planets acquired gases in which the relative xenon abundance was not similar to that of chondrites (*18*). Trapped gases in EET79001 would seem to be relatively unfractionated, with relative abundances similar to those in the atmospheres of Earth and Mars.

Figure 2 is a three-isotope argon correlation plot which permits us to compare argon released from the stepwise degassing of EET79001 samples with possible end-member components of argon, such as the terrestrial atmosphere, the martian atmosphere, and cosmic ray–produced argon. Most of the argon data for one glass and one lith-B whole-rock sample show large $^{40}Ar/^{36}Ar$ ratios of 1300 to 1750 and $^{38}Ar/^{36}Ar$ ratios of 0.28 to 0.36. The feldspar separate, a second lith-B whole rock sample and a second glass sample also show similar trends, but the $^{40}Ar/^{36}Ar$ ratios in these samples are not as large. The highest values of $^{40}Ar/^{36}Ar$ for all of the samples tend to occur at high extraction temperatures where the largest amount ot trapped argon, krypton, and xenon were released. Clearly, trapped argon in these samples contains a component with a high $^{40}Ar/^{36}Ar$ ratio which cannot be due primarily to in situ radiogenic ^{40}Ar or cosmogenic ^{36}Ar. For all samples, data for the lowest extraction temperature (~ 400°C) were relatively small fractions of the total argon, plot near the air point, and probably were adsorbed air. The melt extraction of lith-A whole rock plots between the air value and the region of cosmic ray–produced argon, and probably represents a mixture of these two argon components.

One can correct for cosmic ray–produced argon by assuming that the trapped argon component with a high value of $^{40}Ar/^{36}Ar$ has $^{38}Ar/^{36}Ar = 0.188$, which is the value for the terrestrial atmosphere, is similar to the argon value in chondrites, and apparently is the value for the martian atmosphere to within ±10 percent (*15*). The effects of this correction would be to move each datum leftward and upward as demonstrated for one datum by the dashed line in Fig. 2. The largest observed $^{40}Ar/^{36}Ar$ ratio becomes 2040 when corrected for cosmogenic argon. This value plots only slightly below the lower limit (*15*) for argon in the martian atmosphere and would presumably be a lower limit to the $^{40}Ar/^{36}Ar$ ratio of one major argon component in EET79001.

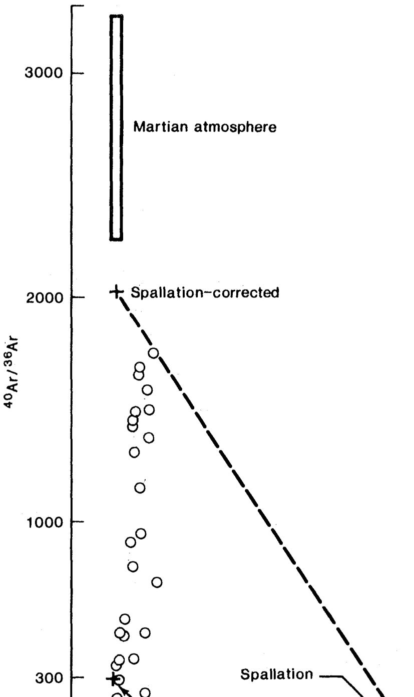

Fig. 2. Isotope correlation plot for argon released from stepwise temperature extractions of six samples of EET79001. Values for the terrestrial atmosphere, the martian atmosphere (*15*), and argon produced by cosmic-ray spallation reactions in silicate material are also shown. The dashed line shows the effects of correcting one measured value for a spallation component.

Argon data from the ~ 800°C extractions of the feldspar and one vesicular glass sample plot substantially below the atmospheric argon point and suggest the presence of a second component with $^{40}Ar/^{36}Ar \leq 131$ and $^{38}Ar/^{36}Ar \simeq 0.2$. This component may have been indigenous to the rock before the shock event, or it may have been acquired from the projectile that caused the shock event. Because we show below that these EET79001 samples contain an appreciable component of krypton and xenon produced by thermal neutron capture on bromine and iodine, it might be expected that argon would show a component produced by thermal neutron capture on chlorine. Such a component, however, should have an $^{38}Ar/^{36}Ar$ ratio of 0.01, which is not consistent with the trend of Fig. 2.

Radiogenic ^{4}He in EET79001 samples occurs in relatively low concentrations (20×10^{-8} to 200×10^{-8} cm^3/g). These data, when combined with uranium and thorium abundances estimated from measured potassium concentrations (*14*) and K/U ratios (*1*, *2*), give ^{4}He gas-retention ages less than the shock age (180 million years). Observed $^{4}He/^{40}Ar$ ratios in those samples with trapped gas were ~ 0.05 to 0.13, whereas the predicted $^{4}He/^{40}Ar$ ratio in SNC meteorites 1300 million years old would be ~ 3.5 and for chondrites 4500 million years old would be ~ 2.5. The substantial fractionation in $^{4}He/^{40}Ar$ compared to predicted decay values probably occurred prior to the introduction of the excess ^{40}Ar component into EET79001, although we cannot rule out the possibility that part of the fractionation occurred during gas escape from the sample. The $^{4}He/^{40}Ar$ ratios in the atmospheres of Earth (0.057) and Mars are also strongly fractionated relative to the predicted values because ^{4}He is not gravitationally bound.

The most striking characteristic of the xenon in EET79001 is the large excesses of ^{129}Xe in those samples that contain trapped gases (Fig. 3). The measured $^{129}Xe/^{136}Xe$ ratios tend to be largest in those high-temperature extractions that released the largest amount of xenon, and the highest observed $^{129}Xe/^{136}Xe$ ratio (5.9) occurred in an extraction of the glass sample that gave the largest total trapped xenon concentration. In contrast, the measured ^{129}Xe/^{136}Xe is nearly "normal" in the total melt extraction of lith-A whole rock, the sample with little, if any, trapped argon. These observations indicate that the excess ^{129}Xe is part of the trapped xenon component in EET79001 rather than from in situ decay of extinct ^{129}I, as is observed in many chondrites and several achondrites which have old ($\sim$ 4500 million years) formation ages. Incorporation of extinct ^{129}I into EET79001 would be highly unlikely because of its very short half-life (16 million years) and the strong indication that shergottites formed by igneous processes only $\sim$ 1300 million years ago. Owen *et al.* reported (*15*) a ^{129}Xe/^{132}Xe ratio for the martian atmosphere of 2.5 (+2, −1). The minimum ^{129}Xe/^{132}Xe ratio for trapped gases in EET79001 would be $\sim$ 2.0, compared to a value for Earth's atmosphere of 0.98. Unfortunately, the Viking experiments were unable to determine other xenon isotopic ratios for the martian atmosphere.

All EET79001 samples (including lith-A whole rock) show appreciable excesses of ^{128}Xe (Fig. 3) and of ^{80}Kr and ^{82}Kr (relative to other krypton isotopes). These excesses cannot be due entirely to spallation because the relative abundances of ^{124}Xe, ^{126}Xe, and ^{78}Kr, which are much more sensitive to a cosmic ray–produced component, are essentially "normal." The ratio of excess ^{80}Kr to excess ^{82}Kr ($\sim$ 3.0) is that predicted for thermal neutron capture on bromine. The excess ^{128}Xe correlates with excess krypton and undoubtedly arises from thermal neutron capture on iodine. The neutron-capture component may have been produced within the sample by cosmic-ray irradiation. The martian atmosphere measured by Viking may also show excesses of ^{80}Kr and ^{82}Kr (*15*). Krypton excesses produced by the secondary neutron component from cosmic rays might be a predictable feature of martian krypton because of the low shielding afforded by the atmosphere (presently $\sim$ 50 g/cm^2) and the likely concentration of halides at the martian surface (*19*).

Possible origins (Table 1) that we have considered for the noble gases contained in EET79001 are (i) gas from the martian atmosphere trapped in EET79001 by the shock event, (ii) trapped gas in chondritic material somehow transferred to EET79001 by collision with or contamination by a chondrite, (iii) adsorbed gas from the terrestrial atmosphere, and (iv) indigenous gas that might be contained in a differentiated asteroidal parent body of EET79001. The relative abundances of neon, argon, krypton, and xenon in EET79001 are essentially the same as those found in the martian and terrestrial atmospheres but distinct from that in chondrites and from that in meteorites containing trapped solar gases (*20*). Association of the trapped noble gases with shock-altered glass and maskelynite indicates that a shock event was responsible for emplacing the trapped gases. Shock can implant a surrounding atmosphere into strongly retentive sites within silicate material without producing appreciable argon isotopic fractionation (*21*). Such evidence is consistent with the idea that trapped gases in EET79001 represent a shock-implanted sample of the martian atmosphere. It is unlikely that trapped gases in EET79001 represent adsorbed terrestrial atmosphere because of their retentive siting and because of the usual tendency of such adsorbed gases to show appreciable elemental fractionation (*18*).

A trapped argon component with ^{40}Ar/^{36}Ar $\gtrsim$ 2040 and trapped xenon with ^{129}Xe/^{132}Xe $\gtrsim$ 2 are also more consistent with what is known about the martian atmosphere than with other possible origins. Although it is conceivable that radiogenic ^{40}Ar could have been acquired from a chondritic contaminant or from an achondritic parent, the latter hypothesis, in particular, seems unlikely because of the presence of other trapped noble gases. The low ^{4}He/^{40}Ar ratio is also inconsistent with a chondritic or achondritic origin without severe gas loss, which could be expected to also fractionate the relative abundances of neon, argon, krypton, and xenon. The young igneous age of SNC meteorites, the apparent lack of a significant ^{129}Xe excess in the lith-A whole rock, and the association of excess ^{129}Xe with trapped xenon rather than with excess ^{128}Xe arising from neutron capture on iodine make it very unlikely that the excess ^{129}Xe formed from in situ decay of ^{129}I. The component produced by neutron capture on halogens in EET79001 could also be consistent with a martian origin, whereas a terrestrial contaminant is ruled out, and an achondritic contaminant seems unlikely in that enhanced halogen abundances may be required.

The characteristics of the various noble gas components within EET79001 samples suggest that the trapped gases in this meteorite are more consistent with an origin from the martian atmosphere than with other possible sources (Table 1). This proposition is largely independent of those petrological, chemical, and chronological data that have been used to infer a martian origin for SNC meteorites (*9*). Strong collisional shock, which produced the glass and maskelynite, would seem to be a reasonable mechanism for implanting martian atmospheric gas into certain phases of EET79001. Such a mechanism would require a relatively high trapping efficiency of $\sim$ 0.2 cm^3 of the present martian atmosphere per gram of glass and may account for the apparent absence of appreciable amounts of such gas in other SNC mete-

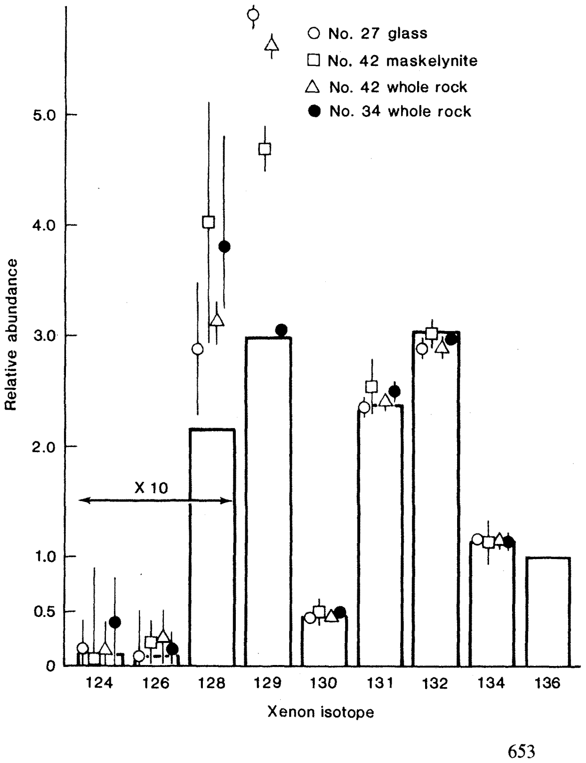

Fig. 3. Relative abundances of xenon isotopes (normalized to ^{136}Xe = 1.0 and the terrestrial atmosphere) for those temperature extractions of four EET79001 samples that released the most total xenon. Measurement uncertainties are shown. The vertical scale for isotopes 124, 126, and 128 has been exaggerated by ×10.

orites. If trapped noble gases in EET79001 were derived from the martian atmosphere, they may have been accompanied by ~ 0.1 part per million (ppm) N_2 and ~ 5 ppm CO_2 (*15*). It will be important to determine the $^{15}N/^{14}N$ ratio in EET79001 because of the large difference between martian and terrestrial N_2 isotopic compositions (*15*). Isotopic measurements of N_2 and CO_2 at these concentrations, however, will be difficult to make.

The presence of trapped martian atmosphere in EET79001, if corroborated by further studies on nonnoble gases, would be a particularly strong argument for the idea that this meteorite is from Mars. The dynamical mechanism required to remove material from a planetary-sized body remains uncertain, although specific mechanisms have been suggested (*22*). The recent identification of another Antarctic meteorite with a probable lunar origin (*23*) suggests that such mechanisms exist. A potential to associate readily available meteoritic material with the martian surface is yet one more demonstration of the value of analytical studies of meteorites to planetary science.

D. D. BOGARD
P. JOHNSON

Planetary and Earth Sciences
Division, NASA Johnson Space
Center, Houston, Texas 77058

References and Notes

1. E. M. Stolper and H. Y. McSween, *Geochim. Cosmochim. Acta* **43**, 1475 (1979); ———, J. F. Hays, *ibid.* **42**, 589 (1978).
2. G. Dreibus *et al.*, *Lunar Planet. Sci.* **13**, 186 (1982).
3. R. N. Clayton and T. K. Mayeda, *Earth Planet. Sci. Lett*, in press.
4. C. Y. Shih *et al.*, *Geochim. Cosmochim. Acta* **46**, 2323 (1982).
5. N. Nakamura, D. M. Unruh, M. Tatsumoto, R. Hutchison, *ibid.*, p. 1555.
6. N. Nakamura, H. Kagami, H. Koni, *Meteoritics*, in press; J. L. Wooden *et al.*, *Lunar Planet. Sci.* **10**, 1379 (1979); N. H. Gale, J. W. Arden, R. Hutchison, *Earth Planet. Sci. Lett.* **26**, 195 (1975); F. A. Podosek, *ibid.* **19**, 135 (1973); D. D. Bogard and L. Husain, *Geophys. Res. Lett.* **4**, 69 (1977); D. A. Papanastassiou and G. J. Wasserburg, *ibid.* **1**, 23 (1974).
7. H. Y. McSween and E. M. Stolper, *Sci. Am.* **242** (No. 6), 54 (1980); J. T. Wasson and G. W. Wetherill, *Asteroids* (Univ. of Arizona Press, Tucson, 1979), p. 926; L. E. Nyquist *et al.*, *Meteoritics* **14**, 502 (1979).
8. H. Y. McSween, Jr., L. A. Taylor, E. M. Stolper, *Science* **204**, 1201 (1979); M. S. Ma, J. C. Laul, R. A. Schmitt, *Proc. Lunar Planet. Sci. Conf.* **12**, 1349 (1981).
9. C. A. Wood and L. D. Ashwal, *Proc. Lunar Planet. Sci. Conf.* **12**, 1359 (1981).
10. W. A. Cassidy, *Antarct. J. U.S.* **15**, 49 (1980).
11. H. Y. McSween and E. Jarosewich, *Lunar Planet Sci.* **13**, 503 (1982).
12. J. Wooden *et al.*, *ibid.*, p. 879.
13. H. Y. McSween and A. M. Reid, *Meteoritics* **16**, 359 (1981).
14. D. D. Bogard, in preparation.
15. T. Owen *et al.*, *J. Geophys. Res.* **82**, 4635 (1977).
16. E. Anders and T. Owen, *Science* **198**, 453 (1977).
17. R. A. Canalas, E. C. Alexander, O. K. Manuel, *J. Geophys. Res.* **73**, 3331 (1968); F. P. Fanale and W. A. Cannon, *Earth Planet. Sci. Lett.* **11**, 362 (1971); ———, T. Owen, *Geophys. Res. Lett.* **5**, 77 (1978).
18. F. A. Podosek, M. Honda, M. Ozima, *Geochim. Cosmochim. Acta* **44**, 1875 (1980).
19. B. C. Clark and D. C. Van Hart, *Icarus* **45**, 370 (1981).
20. L. Schultz and H. Kruse, *Nucl. Track Detection* **2**, 65 (1978); R. O. Pepin and P. Signer, *Science* **149**, 253 (1965).
21. K. Fredriksson, P. DeCarli, R. O. Pepin, J. H. Reynolds, G. Turner, *J. Geophys. Res.* **69**, 1403 (1964); P. K. Davis, *Geochim. Cosmochim. Acta* **41**, 195 (1977).
22. L. E. Nyquist, *Proc. 13th Lunar Planet. Sci. Conf* [*J. Geophys. Res.* **88**, (Suppl.), A785 (1982)]; A. Singer, *Eos* **63**, 1020 (1982).
23. Papers presented at the Special Session on Meteorites from the Earth's Moon, Lunar and Planetary Science Conference, Lunar and Planetary Institute, Houston, 17 March 1983.
24. E. Mazor, D. Heymann, E. Anders, *Geochim. Cosmochim. Acta* **34**, 781 (1970).
25. We thank several of our colleagues, especially L. Nyquist, for constructive comments.

13 December 1982; revised 4 April 1983

Nuclear Magnetic Resonance Blood Flow Measurements in the Human Brain

Abstract. *Timed sequences of nuclear magnetic resonance imaging signals in the human head were used to quantitatively measure blood flow in the internal jugular veins. The procedure can be straightforwardly applied to any vein or artery in the body.*

In this report we describe the use of nuclear magnetic resonance (NMR) techniques to measure blood flow in the human head. In 1959 Singer (*1*) used NMR techniques to study blood flow in mouse tails, and in 1970 Morse and Singer (*2*) obtained NMR measurements of superficial venous flow in humans. Now we can combine NMR imaging systems (*3*) with the measurements of blood flow. The method will be described for two specific vessels in the human head, but it is suitable for any set of arteries or veins or even for blood perfusion measurements.

The procedure for blood flow imaging is as follows. The body is placed in a homogeneous magnetic field. It takes approximately 5 seconds for the protons in the body to be fully magnetized along the magnetic field. A specific volume *V* of the body is selected for flow imaging. A planar cross-sectional volume perpendicular to the flow vessels of interest is the appropriate choice. The selected volume is magnetically depolarized with a radio-frequency (RF) pulse. The RF pulse may be one of several types. We use a pulse to tip the protons in the plane by 90° and follow the pulse with a magnetic field gradient pulse to randomize the proton magnetic orientations in the selected volume. The randomization could also be carried out with a saturating pulse and, in some special procedures, with a 180° pulse. We will refer to all these randomization procedures as the depolarization pulse. After a selected specific time $t(x)$ a second RF pulse is provided. The second pulse tips all the fresh blood protons that entered the selected plane during the time $t(x)$ by 90°. The second pulse also tips the recovered protons that remain in the plane. The tipped magnetic blood protons and recovered stationary protons are then imaged by a spin echo technique (*4–6*), to provide picture elements (pixels) of flow information. Each pixel provides a voltage directly proportional to the volume of blood that flowed into the volume *V*. The computer is programmed to sum the NMR voltages from each pixel in the selected blood vessel and add these voltages to provide the flow data. The tissue recovering from saturation in the volume *V* during the time $t(x)$ gives an imaging signal. These signals do not interfere with the flow measurements because the flow vessels are clearly visualized in the image.

Table 1. Selected flow vessels with tabulated NMR signal intensities for various times of flow. Signal intensity values are proportional to the integrated NMR voltages over the vessel pixels. The data are plotted to evaluate the time required to fill the imaged volume of the vein with inflowing blood. Inflowing blood completely replaces outflowing depolarized blood in 330 msec in the left vein and in 273 msec in the right vein.

Flow time (msec)	Signal intensity	
	Left internal jugular vein	Right internal jugular vein
50	2341	2471
100	3267	3258
200	3885	4340
500	5325	5375

To obtain an accurate measurement of flow, the procedure is repeated several different times. For example, *x* can be 50, 100, 150, and 200 msec. With a computer program the volume flow rate can then be read out for a specific artery or vein. The integrated signals in the vessel are tabulated by the computer, integrated over the vessel area, and indexed with the specific time $t(x)$. The rate of flow of blood in any vessel (milliliters per second) is obtained by dividing